RSC Advances

COMMUNICATION

Cite this: *RSC Adv.*, 2016, **6**, 26199

Received 19th January 2016
Accepted 29th February 2016

DOI: 10.1039/c6ra01599a

www.rsc.org/advances

Zn(II) porphyrin based nano-/microscale metal–organic frameworks: morphology dependent sensitization and photocatalytic oxathiolane deprotection†

Fang-Yao Zhao, Wen-Juan Li, An Guo, Lan Chang, Yue Li* and Wen-Juan Ruan*

With Zn(II) porphyrin as a building block, nano-/microscale MOFs with different morphologies were synthesized as sensitizers for O_2 (forming $^1O_2$). The sensitization efficiency was observed to enhance remarkably with the decrease of morphological dimension of the sample. With high sensitization ability, the one-dimensional MOF could selectively photocatalyze the deprotection of oxathiolanes to ketones.

Emerging as a large group of inorganic–organic hybrid materials, metal–organic frameworks (MOFs) have shown potential application in various fields.[1–6] In particular, a MOF is an ideal platform to construct photocatalysts,[7–9] because chromophores with various structures can be conveniently incorporated into the MOF structure with organic linkers. The inserted chromophores are compactly aligned but not in direct contact with each other, which facilitates light harvesting and energy-transfer processes and prevents self-quenching. The porous structure and large surface area of a MOF photocatalyst also favours its contact with the substrate. Although plenty of MOF photocatalysts have been reported in the literature, most of them were only applied to induce the deep degradation of pollutants.[10–15] In contrast, examples using MOFs to photocatalyze the selective conversion of organics are still rare. Only a handful of reactions, including the oxidation of alcohols (to aldehydes),[6,7] phenols (to quinones),[16,17] sulfides (to sulfoxides)[8,18] and arylboronic acids (to phenols),[19,20] the oxidative coupling of C–C[9,18,20] and C═N[18,20,21] bonds, and the alkylation of aldehydes,[22] have been realized in MOF photocatalytic systems.

To induce the selective transformation of organics, fine control of the excited-state properties of a photocatalyst is required. Using well-studied chromophores as building blocks is a promising strategy to construct selective MOF photocatalysts, because the performance of the obtained MOF photocatalysts in the reaction could be rationally modulated with knowledge about the photophysical properties of the chromophores. Among these chromophores, porphyrin and its derivatives have received particular attention because of their robust structures and unique chemical properties.[6,8,16,20] Additionally, the excited-states of this kind of chromophores exhibit long lifetimes,[23] and can migrate rapidly in the MOF backbone,[24,25] which ensures the high utilization efficiency of light energy.

Aside from composition, the size and shape of MOF photocatalysts, which determine the diffusion distance of the excited-state, would also affect the catalytic efficiency. For example, Lin and co-workers have studied the quenching kinetics of several Ru-bpy based MOF materials, and observed that nearly all the excited states could reach the particle surface to induce the reaction when the particle size was reduced to microscale.[5,26] Although the relationship between the photocatalytic performance and morphology is of great significance for the development of MOF photocatalysis, the comparison among MOF photocatalysts with different morphologies is still lacking.

In this work, with Zn(II) porphyrin as the building block, three nano-/microscale MOF materials (P-1–3) with one to three dimensional morphologies were synthesized. These materials could generate singlet oxygen ($^1O_2$) through a photosensitization process, and the efficiency was enhanced with a decrease of the dimension of the MOF particles. Additionally, taking advantage of the high $^1O_2$ generation ability of the synthesized 1D MOF material, it was used as the photocatalyst to promote the deprotection of oxathiolanes.

The MOF materials were synthesized by the hydrothermal reaction of tetrakis(4-carboxyphenyl)porphyrin (H_2TCPP) with stoichiometric $Zn(NO_3)_2$ and 4,4′-bipyridine (bpy). By the adjustment of reactant concentration, the size and shape of the product could be conveniently modulated. At high reactant concentration (c_{H_2TCPP} = 75 mM), the obtained product (P-1) presents a 1D morphology of square rods (Fig. 1a). The widths of these rods are in the range of 180–240 nm, showing the high

---

Department of Chemistry and Key Laboratory of Advanced Energy Materials Chemistry (Ministry of Education), Nankai University, Tianjin 300071, China. E-mail: wjruan@nankai.edu.cn; liyue84@nankai.edu.cn; Tel: +86-22-23501717

† Electronic supplementary information (ESI) available: Experimental details, TGA curves and structure of MOFs, SEM image of the used photocatalyst, ^{1}H NMR spectra of oxathiolanes, and results of the cyclic experiment. See DOI: 10.1039/c6ra01599a

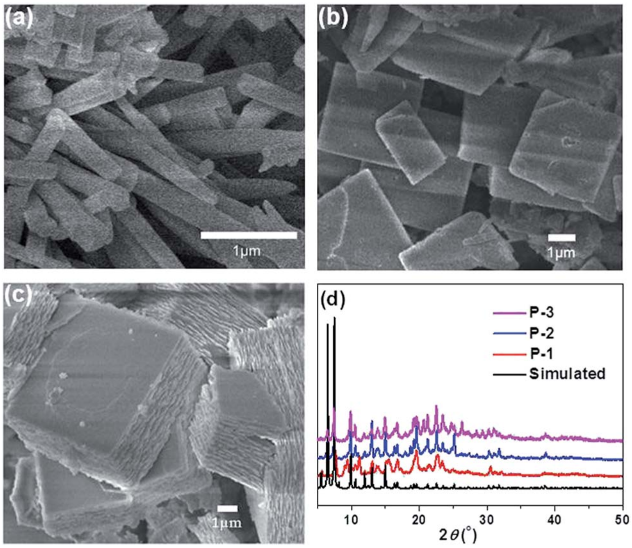

Fig. 1 Typical SEM images of (a) P-1, (b) P-2 and (c) P-3. (d) PXRD patterns of P-1–3. The PXRD patterns and SEM images of the samples obtained by other batches are almost the same as those provided here.

monodispersity of the sample. In contrast, the low concentration of reactants ($c_{\mathrm{H_2TCPP}} = 25$ mM) gave the 2D product (P-2) of square sheets with sides of 3.3–4.8 μm and thicknesses of 130–250 nm (Fig. 1b). The observed change of particle shape is a typical example of the supersaturation dependence of crystal morphology, in which supersaturation, determined by the reactant concentration and working as the driving force for crystallization, controls the preferential growth of crystal surfaces with different energies.[27,28] At a medium reactant concentration ($c_{\mathrm{H_2TCPP}} = 38$ mM), a 3D product of microscale cuboids was formed (Fig. 1c). The layer-by-layer marks on the particles and their square-shaped interface illustrate that the cuboids were assembled by the layered structures of P-2. It is expected that, at this concentration, the critical point for the changing of growth direction is not reached, so the initially formed particles also have the square sheet morphology. A relatively high reactant concentration enhances the amount of sheet formation, reduces the distance between them, and thus facilitates the assembly process to form cuboids. The above observations show that the concentration of reactants has a significant influence on the growth and assembly process of the product, and thus determines the 1D to 3D morphology change.

The coordination structures of P-1–3 were characterized using PXRD (Fig. 1d). Well-defined diffraction peaks recorded in the patterns show the good crystallinity of these samples. The peaks of P-1–3 have close positions, and can be readily indexed to the reported bulk phase of $Zn_3(TCPP)(bpy)_{1.5}$ (Fig. S1, ESI†),[29] indicating that all of our products exhibit the same framework structure. Elemental analysis (EA) showed that P-1–3 have similar chemical compositions with 57.36–57.59% C, 4.41–4.57% H and 9.24–9.28% N. Thermo-gravimetric analysis (TGA) of these samples also gave similar weight loss curves (Fig. S2, ESI†). From room temperature to 700 °C, the overall weight losses of P-1–3 were 86.68%, 84.77% and 83.40%, respectively. Based on the results of EA and TGA, the empirical formula of P-1–3 is defined as $Zn_3(TCPP)(bpy)_{1.5}(DMF)_3(H_2O)_4$ (calcd: 57.45% C, 4.32% H, 9.30% N; weight loss = 83.86%).

Containing the building block of Zn(II) porphyrin, which is a famous chromophore that can sensitize ground state O_2 to the singlet excited-state, P-1–3 are promising to be used as heterogeneous sensitizers for $^1O_2$ generation. The photosensitizing abilities of these MOF materials were evaluated in their O_2 saturated suspensions of acetonitrile, and 1,3-diphenylisobenzofuran (DPBF) was used as the probe to capture the produced $^1O_2$ (Fig. 2). A 500 W halogen lamp was used as the light source, and light below 450 nm was cut off to prevent the photolysis of DPBF (curve 1 of Fig. 2a). In the presence of P-1, the absorption of DPBF gave a rapid decrease and nearly vanished in 180 s under irradiation (curve 2). The fitting of the degradation plots of DPBF gives the $^1O_2$ generation rate constant of 2.5×10^{-3} s^{-1}, showing that the sensitization efficiency of P-1 is among the best recently reported MOF sensitizers.[30–32] P-2 and P-3 could also markedly degrade DPBF (curves 3 and 4), but the rates ($k_{\text{P-2}} = 1.1 \times 10^{-3}$ s^{-1} and $k_{\text{P-3}} = 0.5 \times 10^{-3}$ s^{-1}) were much lower than that of P-1. The higher sensitization efficiency of P-1 could be explained by its 1D morphology, which magnifies the external surface of particles and thus favours the contact with O_2. After the photosensitization processes, the sensitizers were removed from the reaction media by filtration, and DPBF was supplemented to the filtrates to the original concentration. The further irradiation of the filtrates caused negligible change on the absorption of DPBF (curves 5–7), implying that the O_2 sensitization processes of P-1–3 are heterogeneous in nature and not due to components leaching into the solution.

The $^1O_2$ generation ability of P-1 was further confirmed with an electron spin resonance (ESR) method. It has been established that 2,2,6,6-tetramethylpiperidine (TMP) reacts with $^1O_2$ to form a stable nitroxide radical (TMPO), which can be recorded by ESR spectroscopy.[33,34] The suspension containing P-1 and TMP was filled into a quartz capillary, and irradiated *in situ*. As shown in Fig. 3a, after only 2 s of irradiation, the typical signal of TMPO (threefold peaks with intensities of 1 : 1 : 1) appeared. The intensity of this signal enhanced linearly with

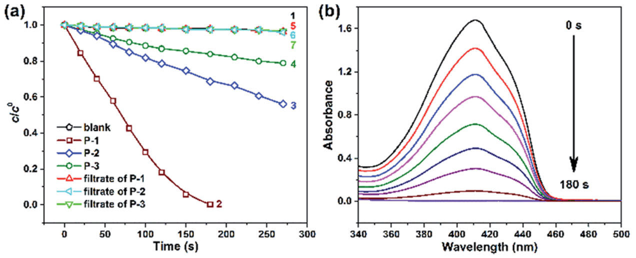

Fig. 2 (a) Absorbance decay of the reacted DPBF solution at 410 nm under different conditions. (b) The change of the absorption spectrum of the reacted DPBF solution with P-1 as a sensitizer. 20 mg of sensitizer, $c^0_{\mathrm{DPBF}} = 60$ μM, 100 mL of acetonitrile, with O_2 bubbled though the reaction, spectra were recorded after the separation of the sensitizer.

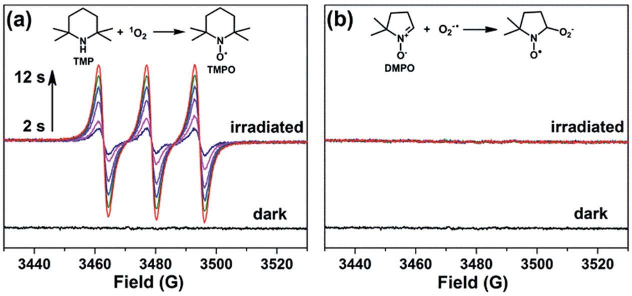

Fig. 3 (a) ESR spectra of the acetonitrile suspension containing P-1 (1 g L^{-1}) and TMP (40 mM). (b) ESR spectra of the methanol suspension containing P-1 (1 g L^{-1}) and DMPO (40 mM). The suspensions were scanned after 0, 2, 4, 6, 8, 10 and 12 s of irradiation (355 nm).

prolonged irradiation time (Fig. S3, ESI†), which definitely corroborates the photosensitized formation of $^1O_2$. Aside from sensitization, it is also possible to activate O_2 through the electron-transfer process to form superoxide ($O_2^{-\bullet}$). The potential formation of $O_2^{-\bullet}$ was also tested by ESR (with 5,5-dimethyl-1-pyrroline-*N*-oxide (DMPO) as a spin trapper).[35,36] This experiment was carried out in methanol, which also works as the electron donor. In contrast to the rapid formation of $^1O_2$, no resonance signal was recorded after 12 s of irradiation in this experiment (Fig. 3b). These results indicate that P-1 only activates O_2 through the sensitization process and can be used as a pure sensitizer to generate $^1O_2$.

The transformation of oxathiolanes to ketones is extremely important in organic synthesis because oxathiolane is a widely used protecting group for carbonyls.[37,38] This reaction was traditionally induced with stoichiometric reagents, such as mercuric cyanide,[39] iodonium dicollidine perchlorate,[40] RANEY® Ni,[41] SeO_2/H_2O_2 (ref. 42) and glyoxylic acid.[43] Recently, Lamb and co-workers reported a homogeneous photocatalytic system to induce this transformation, in which $^1O_2$ generated from the sensitization of molecular dyes works as the main active species.[44] Considering the $^1O_2$ generation ability of P-1, we used it as a heterogeneous photocatalyst to promote this reaction. The photocatalytic reactions were carried out in an acetonitrile suspension containing P-1 and **1a** under the irradiation of visible light (from a 300 W Xe lamp cutoff below 420 nm). The substrate was consumed completely in 90 min, and nearly quantitatively transformed to acetophenone (Table 1, entry 1). Control experiments showed that P-1, O_2, and light irradiation are all necessary for this reaction (entries 2–4). To characterize the reusability of P-1, a cyclic experiment was carried out. At the end of each cycle, the photocatalyst was separated with centrifugation, washed thoroughly, and reused for the next run. The photocatalytic ability of P-1 was maintained after six experimental cycles with no remarkable loss of activity or selectivity (Table 1, entry 5 and Table S1, ESI†). Based on the determined formula of $Zn_3(TCPP)(bpy)_{1.5}(DMF)_3(H_2O)_4$ ($M_w = 1505$), the total turnover number (TON) of six cycles was 450, which explicitly proves that P-1 works as a photocatalyst in this reaction. SEM observation revealed that the morphology of the used catalyst was nearly identical with that of the as-prepared one (Fig. S4, ESI†), showing the high stability of P-1 in the reaction system.

Table 1 Photocatalytic deprotection of oxathiolanes to ketones by P-1[a]

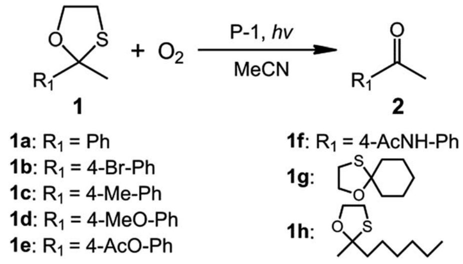

Entry	Substrate	Time (min)	Conv. (%)	Sel.[b] (%)
1	**1a**	90	100	95
2[c]	**1a**	90	0	—
3[d]	**1a**	90	0	—
4[e]	**1a**	90	0	—
5[f]	**1a**	90	99	96
6	**1b**	90	97	99
7	**1c**	90	99	82
8	**1d**	110	100	86
9	**1e**	100	100	>99
10	**1f**	110	97	84
11	**1g**	90	100	>99
12	**1h**	90	100	>99

[a] Reaction conditions: 2 mg P-1, 50 mM oxathiolane, 2 mL of acetonitrile, 1 atm of O_2 300 W Xe lamp cutoff below 420 nm. [b] Determined by GC with bromobenzene as an internal standard. [c] Without irradiation. [d] In N_2 atmosphere. [e] Without P-1. [f] The results of the sixth reaction cycle.

To test the applicability of this reaction, other aryloxathiolanes (**1b–1f**) were used as substrates. Similar to **1a**, all of these substrates could be smoothly transformed to the corresponding ketones in the photocatalytic system of P-1 with selectivity greater than 80% (entries 6–10). We further extend the substrate scope to alkyloxathiolanes, and observed that the photocatalytic deprotections of **1g** and **1h** were also nearly quantitative (entries 11 and 12). These results are in contrast to those of the reaction system reported by Lamb *et al.*, in which the yield of the ketone product is minimal in the absence of an aryl substrate.[44] The high selectivity of alkyloxathiolane deprotection in our photocatalytic system may be due to that P-1 only activates O_2 through the energy-transfer process to form $^1O_2$ (Fig. 3), and thus prevents the side reactions induced by other reactive oxygen species.

Conclusions

In summary, Zn(II) porphyrin based nano-/microscale MOF materials were synthesized under solvothermal conditions in this work. Reactant concentration was proven to play a significant role in the growth and assembly of MOF particles. With the enhancement of reactant concentration, the MOF products with 2D (square sheet), 3D (layered cuboid) and 1D (square rod) morphologies were obtained in sequence. These MOF materials could be used as heterogeneous sensitizers for the generation of $^1O_2$, and the efficiency enhanced with the decrease of particle dimension. Taking advantage of the $^1O_2$ generation ability, a photocatalytic method was developed for the deprotection of oxathiolanes to ketones, and a high reaction rate and selectivity were observed. To the best of our knowledge, this is the first time of realizing oxathiolane deprotection in the photocatalytic system of MOFs. The results of this work illustrate the morphology–function relationship of MOF sensitization, and extend the reaction scope of MOF photocatalysis.

Acknowledgements

This work is supported by the National Natural Science Foundation of China (21307062, 20671053) and Tianjin Research Program of Application Foundation and Advanced Technology (14JCQNJC08000).

Notes and references

1 M. P. Suh, H. J. Park, T. K. Prasad and D.-W. Lim, *Chem. Rev.*, 2012, **112**, 782–835.

2 L. E. Kreno, K. Leong, O. K. Farha, M. Allendorf, R. P. Van Duyne and J. T. Hupp, *Chem. Rev.*, 2012, **112**, 1105–1125.

3 V. Stavila, A. A. Talin and M. D. Allendorf, *Chem. Soc. Rev.*, 2014, **43**, 5994–6010.

4 J. Liu, L. Chen, H. Cui, J. Zhang, L. Zhang and C.-Y. Su, *Chem. Soc. Rev.*, 2014, **43**, 6011–6061.

5 C. A. Kent, D. Liu, L. Ma, J. M. Papanikolas, T. J. Meyer and W. Lin, *J. Am. Chem. Soc.*, 2011, **133**, 12940–12943.

6 S. Yuan, T.-F. Liu, D. Feng, J. Tian, K. Wang, J. Qin, Q. Zhang, Y.-P. Chen, M. Bosch, L. Zou, S. J. Teat, S. J. Dalgarno and H.-C. Zhou, *Chem. Sci.*, 2015, **6**, 3926–3930.

7 L. Shen, S. Liang, W. Wu, R. Liang and L. Wu, *J. Mater. Chem. A*, 2013, **1**, 11473–11482.

8 J. A. Johnson, X. Zhang, T. C. Reeson, Y.-S. Chen and J. Zhang, *J. Am. Chem. Soc.*, 2014, **136**, 15881–15884.

9 D. Shi, C. He, B. Qi, C. Chen, J. Niu and C. Duan, *Chem. Sci.*, 2015, **6**, 1035–1042.

10 L. Ai, C. Zhang, L. Li and J. Jiang, *Appl. Catal., B*, 2014, **148**, 191–200.

11 K. G. M. Laurier, F. Vermoortele, R. Ameloot, D. E. De Vos, J. Hofkens and M. B. J. Roeffaers, *J. Am. Chem. Soc.*, 2013, **135**, 14488–14491.

12 P. Du, Y. Yang, J. Yang, B.-K. Liu and J.-F. Ma, *Dalton Trans.*, 2013, **42**, 1567–1580.

13 J. Gao, J. Miao, P.-Z. Li, W. Y. Teng, L. Yang, Y. Zhao, B. Liu and Q. Zhang, *Chem. Commun.*, 2014, **50**, 3786–3788.

14 A. Wang, Y. Zhou, Z. Wang, M. Chen, L. Sun and X. Liu, *RSC Adv.*, 2016, **6**, 3671–3679.

15 Z. Zhang, X. Li, B. Liu, Q. Zhao and G. Chen, *RSC Adv.*, 2016, **6**, 4289–4295.

16 J. Park, D. Feng, S. Yuan and H.-C. Zhou, *Angew. Chem., Int. Ed.*, 2015, **54**, 430–435.

17 M.-H. Xie, X.-L. Yang, C. Zou and C.-D. Wu, *Inorg. Chem.*, 2011, **50**, 5318–5320.

18 C. Wang, Z. Xie, K. E. deKrafft and W. Lin, *J. Am. Chem. Soc.*, 2011, **133**, 13445–13454.

19 X. Yu and S. M. Cohen, *Chem. Commun.*, 2015, **51**, 9880–9883.

20 J. A. Johnson, J. Luo, X. Zhang, Y.-S. Chen, M. D. Morton, E. Echeverría, F. E. Torres and J. Zhang, *ACS Catal.*, 2015, **5**, 5283–5291.

21 X. Qiu, C. Len, R. Luque and Y. Li, *ChemSusChem*, 2014, **7**, 1684–1688.

22 P. Wu, C. He, J. Wang, X. Peng, X. Li, Y. An and C. Duan, *J. Am. Chem. Soc.*, 2012, **134**, 14991–14999.

23 B. Marydasan, A. K. Nair and D. Ramaiah, *J. Phys. Chem. B*, 2013, **117**, 13515–13522.

24 H.-J. Son, S. Jin, S. Patwardhan, S. J. Wezenberg, N. C. Jeong, M. So, C. E. Wilmer, A. A. Sarjeant, G. C. Schatz, R. Q. Snurr, O. K. Farha, G. P. Wiederrecht and J. T. Hupp, *J. Am. Chem. Soc.*, 2013, **135**, 862–869.

25 M. C. So, S. Jin, H.-J. Son, G. P. Wiederrecht, O. K. Farha and J. T. Hupp, *J. Am. Chem. Soc.*, 2013, **135**, 15698–15701.

26 C. A. Kent, D. Liu, T. J. Meyer and W. Lin, *J. Am. Chem. Soc.*, 2012, **134**, 3991–3994.

27 X. Lu, X. Wang, Q. Liao and H. Fu, *J. Phys. Chem. C*, 2015, **119**, 22108–22113.

28 S. X. M. Boerrigter, H. M. Cuppen, R. I. Ristic, J. N. Sherwood, P. Bennema and H. Meekes, *Cryst. Growth Des.*, 2002, **2**, 357–361.

29 E.-Y. Choi, P. M. Barron, R. W. Novotny, H.-T. Son, C. Hu and W. Choe, *Inorg. Chem.*, 2009, **48**, 426–428.

30 Y. Liu, A. J. Howarth, J. T. Hupp and O. K. Farha, *Angew. Chem., Int. Ed.*, 2015, **54**, 9001–9005.

31 K. Lu, C. He and W. Lin, *J. Am. Chem. Soc.*, 2014, **136**, 16712–16715.

32 L. Zhang, J. Lei, F. Ma, P. Ling, J. Liu and H. Ju, *Chem. Commun.*, 2015, **51**, 10831–10834.

33 Y. Lion, M. Delmelle and A. Van De Vorst, *Nature*, 1976, **263**, 442–443.

34 J. Moan and E. Wold, *Nature*, 1979, **279**, 450–451.

35 F. A. Villamena, J. K. Merle, C. M. Hadad and J. L. Zweier, *J. Phys. Chem. A*, 2005, **109**, 6089–6098.

36 J.-L. Clément, N. Ferré, D. Siri, H. Karoui, A. Rockenbauer and P. Tordo, *J. Org. Chem.*, 2005, **70**, 1198–1203.

37 G. Sartori, R. Ballini, F. Bigi, G. Bosica, R. Maggi and P. Righi, *Chem. Rev.*, 2004, **104**, 199–250.

38 G. E. Wilson, M. G. Huang and W. W. Schloman, *J. Org. Chem.*, 1968, **33**, 2133–2134.

39 J. O. Kihlberg, D. A. Leigh and D. R. Bundle, *J. Org. Chem.*, 1990, **55**, 2860–2863.

40 G. H. Veeneman and J. H. van Boom, *Tetrahedron Lett.*, 1990, **31**, 275–278.

41 C. Djerassi, M. Shamma and T. Y. Kan, *J. Am. Chem. Soc.*, 1958, **80**, 4723–4732.

42 T. Mandai, M. Takeshita, M. Kawada and J. Otera, *Chem. Lett.*, 1984, **13**, 1259–1260.

43 S. P. Chavan, P. Soni and S. K. Kamat, *Synlett*, 2001, **2001**, 1251–1252.

44 B. M. Lamb and C. F. Barbas Iii, *Chem. Commun.*, 2015, **51**, 3196–3199.